PHYSICAL REVIEW A

GENERAL PHYSICS

THIRD SERIES, VOLUME 28, NUMBER 4 OCTOBER 1983

Stark effect in barium $6snd\ ^1D_2$ Rydberg states; evidence of strong perturbations in the $^1F_3$ series

K. A. H. van Leeuwen,* W. Hogervorst, and B. H. Post

Natuurkundig Laboratorium der Vrije Universiteit, De Boelelaan 1081, 1081 HV Amsterdam, The Netherlands

(Received 25 April 1983)

The scalar and tensor polarizabilities of the barium $6snd\ ^1D_2$ states with principal quantum number n ranging from 14 to 30, as well as those of the $5d7d\ ^1D_2$ perturber state near $n=26$, have been measured with high-resolution laser—atomic-beam spectroscopy. The data are analyzed by calculating the contribution to the polarizabilities of all known odd-parity states connected via the electric dipole operator with the $^1D_2$ states. In this way the contributions of the unknown $6snf\ ^1F_3$ states are inferred. The results indicate that the $^1F_3$ series is heavily affected by at least two perturber states. A tentative three-channel quantum-defect—theory analysis of the $^1F_3$ series, based on a fit to the experimental polarizabilities, is presented.

I. INTRODUCTION

The highly excited states of atomic barium below the first ionization limit have been the subject of many recent investigations. Extensive measurements of the energies of the even-parity states with total angular momentum J up to five have been performed.[1–4] Analyses in terms of multichannel quantum-defect theory (MQDT) by Aymar *et al.*[3,5,6] indicate that the $6sns$, $6snd$, and $6sng$ Rydberg states are perturbed by many doubly excited states belonging to $6pnp$, $5dns$, and $5dnd$ configurations.

The wave functions resulting from the MQDT analyses, especially those for the $J=0$ and 2 states, have been subjected to a number of experimental tests including lifetime measurements,[7–9] Stark-shift measurements,[8] g_j-factor determinations,[10] isotope shift measurements,[11] and hyperfine-structure data.[11–15] The MQDT wave functions generally prove to be adequate. However, the $J=2$ analysis had to be extended[10,14–16] to include the direct interaction between the $6snd\ ^1D_2$ and $6snd\ ^3D_2$ states, which is impossible to deduce from the level energies but is clearly reflected in the Zeeman effect and hyperfine-structure data.

Less exhaustive data are available on the odd-parity states. The energies of the $6snp$ states with $J=1$ and 2 and associated perturber states (belonging to $5dnp$ and $5dnf$ configurations) have been measured by Armstrong *et al.*[17] who performed an extensive MQDT analysis of their results. The $J=1$ states have been treated in an eight-channel analysis, whereas a two-channel treatment sufficed for the weakly perturbed $^3P_2$ series. Only a few highly excited odd-parity states with $J=0$ are known.[17]

The $6snf$ Rydberg series are of special interest in this paper. The energies of the ^3F states up to principal quantum number $n=32$ are given by Carlsten *et al.*,[18] partly citing unpublished data of Camus and Tomkins. For a number of $^3F_2$ and $^3F_3$ states with n ranging from 9—55, the level energies have been accurately determined by Armstrong *et al.*[17] and by Eliel and Hogervorst.[19] The ^3F series appear to be unperturbed above $n=12$ apart from a weak perturbation at $n=20$ in the $^3F_2$ (Refs. 17 and 19) and possibly also in the $^3F_4$ series.[18] For the $^3F_2$ and $^3F_3$ series this conclusion has been confirmed by the hyperfine-structure measurements of Eliel and Hogervorst.[19] Data on the $6snf\ ^1F_3$ level energies for n larger than 9 are scarce. In Ref. 19 results for $n=40$, 45, and 50 are reported, and Gallagher *et al.*[8] give a value for the $6s24f\ ^1F_3$ state. However, the assignment of the latter state has been questioned, as it appears to be incompatible with the hyperfine structure of the $6s24f\ ^3F$ states in the odd isotopes.[19]

Measurements of the quadratic Stark effect in the even-parity $^1D_2$ states can, in principle, supply information both on the $^1D_2$ states themselves and on the nearby odd-parity $J=1$, 2, and 3 states, which contribute to the $^1D_2$ polarizabilities via the electric dipole operator. The uncommon situation that extensive data exist on the energies and wave functions of all states involved, except the odd-parity $^1F_3$ states, provides the opportunity to extract information on the latter states from the polarizabilities of the $^1D_2$ states. This information is not only useful to complete the picture of barium as a showcase of MQDT, but also to validate the treatment of the hyperfine structure in the ^3F Rydberg states in terms of a small number of physically meaningful parameters as given in Ref. 19.

Tensor polarizabilities of the $6snd\ ^1D_2$ states with principal quantum numbers 15—18 and 22 have been measured by Fechner *et al.*[20] using quantum-beat spectros-

copy. Their polarizabilities roughly scale with the sixth power of the effective principal quantum number and agree reasonably well with calculations based on the Coulomb approximation of Bates and Damgaard,[21] taking into account only the contributions of the $6snp\ ^1P_1$ states. The Stark effect in the $5d7d\ ^1D_2$ state, which perturbs the $6snd\ ^1D_2$ states around $n=26$, has been studied by Gallagher *et al.*[8] They observed radio-frequency transitions to levels designated $6s28s\ ^1S_0$, $6s24f\ ^3F_2$, and $6s24f\ ^1F_3$ in a weak electric field (up to a few V/cm). However, if the $^1F_3$ level has indeed been erroneously assigned, their interpretation of the results is not valid. Finally, Zimmerman *et al.*[22] studied the Stark effect of Rydberg states in the vicinity of effective principal quantum number $n^*=12$ in strong electric fields (up to 10 kV/cm). As at that time no detailed MQDT analyses of barium level energies were available, their interpretation of the experimental data was limited.

In this paper the results of measurements of the scalar and tensor polarizabilities of the $6s14d$–$6s30d\ ^1D_2$ states and of the $5d7d\ ^1D_2$ perturber state, using high-resolution laser–atomic-beam spectroscopy, will be presented.

II. EXPERIMENTS AND RESULTS

A detailed description of the experimental setup is presented elsewhere,[15,19] therefore, only a brief description, stressing details pertinent to the present experiment, is given here. Barium atoms in a well-collimated beam are excited to high-lying $^1D_2$ levels by two-step excitation from the $6s^2\ ^1S_0$ ground state via the $6s6p\ ^1P_1$ intermediate state. Two frequency-stabilized single-mode cw dye lasers are used. A Spectra Physics 580 linear laser operating on the dye Rhodamine-110 excites the first transition ($6s^2\ ^1S_0 \rightarrow 6s6p\ ^1P_1$ at 553.5 nm) and is locked in frequency on the center of the ^{138}Ba excitation. For this purpose the fluorescent light is detected in a separate interaction region. A Spectra Physics 380 D ring laser operating on the dye Stilbene-3 is scanned over the excitation profile of the second transition ($6s6p\ ^1P_1 \rightarrow 6snd\ ^1D_2$, 420–433 nm). In contrast with broadband excitation of the first step, the structure of the intermediate level is not reflected in the recorded excitation profile.

The interaction region of the laser beams and the atomic beam is centered between two field plates (one stainless-steel plate and one copper mesh electrode) sustaining the electric field. The excited atoms are field ionized 2-cm downstream and the detached electrons are detected by an electron multiplier. During a laser scan, the electron-multiplier signal and the signal of a calibration interferometer which provides the frequency scale are stored by an on-line minicomputer.

In the absence of external fields, the excitation spectrum of the isotope ^{138}Ba (natural abundancy 71.7%, nuclear spin $I=0$) consists of a single peak. In an electric field this peak is split into three components corresponding to the excited-state sublevels with $|M|=0$, 1, and 2 (M is the magnetic quantum number). In the low-field limit, the shift of each sublevel is quadratic in the electric-field strength. The splittings $|M|=2-|M|=1$ and $|M|=1-|M|=0$ are in the ratio of 3:1. However, at the field strengths used (up to 50 V/cm for the $6s14d\ ^1D_2$ state and up to 16 V/cm for the $6s30d\ ^1D_2$ state) deviations from the quadratic Stark effect and the splitting rule were observed. This has been accounted for by fitting the shifts with the sum of a quadratic and a fourth-power term, which is the first higher-order term resulting from the perturbational treatment of the Stark effect. The polarizabilities are then determined from the quadratic terms. The effect of contact potentials between the field plates, effectively causing a bias field which was not completely constant during the experiments, has been corrected for by performing all measurements also with the polarity of the field reversed.

The resulting values for the scalar polarizabilities (α_0) and tensor polarizabilities (α_2) are given in Table I. The earlier results of Fechner *et al.*[20] are indicated and are in good agreement with the present data. The errors are composed of the tripled statistical error in the determination of the polarizabilities and a systematic error of 3% due to the calibration of the distance between the field plates. The labels of the levels are given according to Aymar,[3] but it should be remarked that the level at 41 831.90 cm^{-1} has been relabeled $6s26d\ ^3D_2$ in later analyses.[14,16]

Since in the hydrogenic model[23] the polarizabilities of Rydberg states scale with $(n^*)^7$, a convenient way of representing the polarizabilities graphically is to plot $\alpha_0/(n^*)^7$ and $\alpha_2/(n^*)^7$ against n^*. The experimental results are plotted in this way in Fig. 1 (the connecting lines only serve to guide the eye). A highly irregular behavior is observed, thwarting any attempt to state even an approximate power law.

III. DISCUSSION

A. General

The shift induced by a weak electric field E_z in the energy of an atomic (sub)state with total angular moment J and magnetic quantum number M is given by[24]

$$\Delta W = \left[-\tfrac{1}{2}\alpha_0^{\gamma J} - \tfrac{1}{2}\alpha_2^{\gamma J} \frac{3M^2 - J(J+1)}{J(2J-1)} \right] E_z^2 . \tag{1}$$

This equation defines the scalar polarizability α_0 and the tensor polarizability α_2. The polarizabilities can be expressed in reduced matrix elements of the electric dipole operator $\vec{P}$ as follows:

$$\alpha_0^{\gamma J} = \frac{-2}{3(2J+1)} \sum_{\gamma' J'} \frac{|\langle \gamma J || \vec{P} || \gamma' J' \rangle|^2}{W_{\gamma J} - W_{\gamma' J'}} , \tag{2}$$

and

$$\alpha_2^{\gamma J} = -2\left(\tfrac{10}{3}\right)^{1/2} \left[\frac{J(2J-1)}{(2J+3)(J+1)(2J+1)} \right]^{1/2} (-1)^{2J} \sum_{\gamma' J'} (-1)^{J-J'} \begin{Bmatrix} J & J' & 1 \\ 2 & 2 & J \end{Bmatrix} \frac{|\langle \gamma J || \vec{P} || \gamma' J' \rangle|^2}{W_{\gamma J} - W_{\gamma' J'}} , \tag{3}$$

TABLE I. Experimental polarizabilities for $^1D_2$ states in barium. The errors correspond to three times the statistical error combined with an estimated 3% (systematic) error due to the calibration of the electric field. The results of Fechner *et al.* (Ref. 20) are shown in the last column.

Level energy (cm^{-1})	Designation	Polarizabilities [MHz/(V/cm)^2] Scalar (this expt)	Tensor (this expt)	Tensor [other (Ref. 20)]
41 162.34	14^1D_2	−0.515(20)	−0.371(17)	
41 315.40	15^1D_2	−0.0819(27)	0.0871(26)	0.0885(22)
41 417.40	16^1D_2	−0.131(4)	0.142(4)	0.144(5)
41 500.14	17^1D_2	−0.205(9)	0.218(9)	0.213(7)
41 567.28	18^1D_2	−0.281(12)	0.325(11)	0.328(8)
41 622.58	19^1D_2	1.53(5)	−0.080(24)	
41 668.64	20^1D_2	−0.636(20)	0.684(22)	
41 707.39	21^1D_2	−0.680(26)	0.89(3)	
41 740.28	22^1D_2	−0.316(15)	1.04(3)	1.10(4)
41 768.42	23^1D_2	3.75(11)	0.101(5)	
41 792.65	24^1D_2	−10.7(3)	4.55(14)	
41 813.62	25^1D_2	−8.81(26)	4.11(14)	
41 831.90	26^1D_2	−12.8(4)	4.07(13)	
41 841.55	$5d\,7d\ ^1D_2$	19.2(6)	−3.33(18)	
41 851.92	27^1D_2	−0.876(28)	0.895(28)	
41 864.69	28^1D_2	−4.44(14)	3.14(9)	
41 876.99	29^1D_2	−7.1(3)	4.99(28)	
41 888.18	30^1D_2	−9.6(3)	6.65(21)	

in which γ denotes all quantum numbers apart from J and M which are necessary to describe a state. The sums extend over all electronic states (including continuum states) with parity opposite to the parity of the state under consideration. However, due to the energy denominators and the properties of the dipole matrix elements, a small number of neighboring states usually dominates the sums in expressions (2) and (3). In order to evaluate α_0 and α_2, we can thus restrict ourselves to the contributions of the nearby opposite-parity states which satisfy the $|\Delta J| \leq 1$ selection rule for the dipole matrix elements. The knowledge of wave functions and energies of all levels involved is then required to calculate the matrix elements and, subsequently, the polarizabilities. The specification of wave functions in a basis of MQDT channels is generally sufficient to reduce the dipole matrix elements to the appropriate single-electron radial integrals

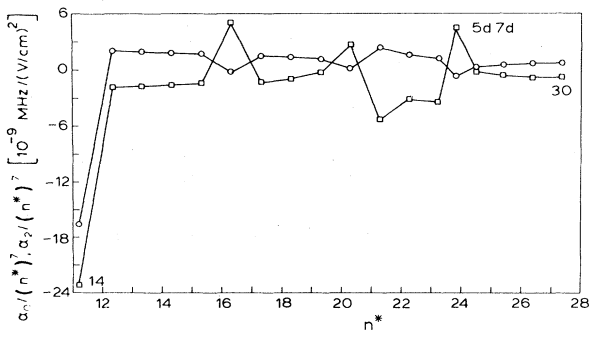

FIG. 1. Scalar (□) and tensor (○) polarizabilities divided by $(n^*)^7$ (n^* is effective principal quantum number) as a function of n^* for barium $^1D_2$ states.

$$R^{nl}_{n'l'} = \int_0^\infty R_{nl}(r) r R_{n'l'}(r) r^2 dr \ , \tag{4}$$

in which $R_{nl}(r)$ is the radial wave function of the nl electron.

For highly excited states, the radial integrals are usually calculated in the Coulomb approximation, assuming generalized hydrogenic radial functions which are normalized to the experimental level energies.[21] This approximation is expected to give good results for Rydberg states, as the major contribution to the integral $R^{nl}_{n'l'}$ stems from large values of r.

The restriction to a small number of opposite-parity states and the use of the Coulomb approximation may introduce errors in the calculation of the polarizabilities. These can be estimated from a comparison of experimental and calculated polarizabilities of (almost) unperturbed Rydberg states. In a separate article[25] we report experimental and calculated values of the polarizabilities of calcium $4sns\ ^3S_1$ and $4snd\ ^3D_{1,2,3}$ Rydberg states. The results agree to within a few percent, generally well within the experimental error.

B. Calculation of the $^1D_2$ polarizabilities (without the $^1F_3$ contributions)

In the analysis of the polarizabilities of the $^1D_2$ states, the contributions of the odd-parity $J=1$, 2, and 3 levels in the energy region 40 500–41 925 cm^{-1} (corresponding to n^* between 8 and 32) have been considered.

Wave functions and energies of the $^1D_2$ states themselves have been derived from the parameter set of Aymar's modified nine-channel MQDT analysis.[16] The odd-parity $J=1$ states have been evaluated according to the eight-channel analysis of Armstrong *et al.*[17] who also supplied the two-channel parameters for the $^3P_2$ series.

The $6snf\,^3F_2$ series, which does not show any perturbation except a weak one at $n=20$, has been derived from a pure one-channel fit (with linearly energy-dependent quantum defect) to level energies measured by Armstrong *et al.*[17] and by Eliel and Hogervorst.[19] For $n=20$, the experimental level energy has been substituted. The $^3F_3$ series was also taken to be pure $6snf\,^3F_3$; the energies were determined by graphical interpolation of a quantum defect versus n plot of levels measured by Carlsten *et al.*[18] and by Eliel and Hogervorst.[19] The $^3F_3$ series shows a perturbation around $n=11$, but appears to be completely unperturbed for $n>16$.

The pure triplet states ($^3P_2$, $^3F_2$, and $^3F_3$) only contribute to the polarizabilities of the $^1D_2$ states insofar as these are mixed with triplet states; this concerns the $6s14d\,^1D_2$ state and those around $n=26$.

With these data the contributions of all odd-parity states discussed to the polarizabilities have been calculated. The $^1F_3$ states have been omitted at this stage. We therefore write the polarizabilities of the $^1D_2$ states:

$$\begin{aligned}\alpha_0&=\alpha_0(^1F_3)+\alpha_0(\text{rest})\ ,\\ \alpha_2&=\alpha_2(^1F_3)+\alpha_2(\text{rest})\ ,\end{aligned}\tag{5}$$

and designate the sums of the calculated contributions $\alpha_0^{\text{calc}}(\text{rest})$ and $\alpha_2^{\text{calc}}(\text{rest})$.

The one-electron radial integrals $R^{nl}_{n'l'}$ have been determined with the procedure described by Zimmerman *et al.*[26,27] which is based on the direct numerical solution of the Coulombic radial equations. Only those contributions to the polarizabilities which involve a change in effective principal quantum number of the active electron smaller than five have been considered. This corresponds to a cut-off criterium in energy difference as discussed in Sec. III A, which is justified both by the energy denominators in Eqs. (2) and (3) and by the fact that the radial integrals $R^{nl}_{n'l'}$ decrease very rapidly with increasing Δn^* $[=|n^*(n,l)-n^*(n',l')|]$. As a test, some of the calculations have been repeated with a $\Delta n^*<2$ criterium. The results differ less than 1% from those obtained with $\Delta n^*<5$ indicating the latter criterium to be on the safe side.

The results of the calculations of $\alpha_0(\text{rest})$ and $\alpha_2(\text{rest})$ are given in Table II. For the levels designated $6s14d\,^1D_2$ and $5d7d\,^1D_2$, the uncertainty in the calculations is large. These levels are nearly degenerate with the $6s15p\,^3P_2$ and $6s24f\,^3F_2$ levels, respectively, and the error in energy separation is comparable to the separation itself. For this reason these two levels have not been considered in further analysis.

For the remaining states, the differences $\Delta\alpha_0=\alpha_0^{\text{expt}}-\alpha_0^{\text{calc}}(\text{rest})$ and $\Delta\alpha_2=\alpha_2^{\text{expt}}-\alpha_2^{\text{calc}}(\text{rest})$ [see Eq. (5)] are assumed to be the contributions of the $^1F_3$ states $\alpha_0(^1F_3)$ and $\alpha_2(^1F_3)$, respectively. This assumption can be tested by comparing $\Delta\alpha_0$ and $\Delta\alpha_2$ for each $^1D_2$ state. From Eqs. (2) and (3) it can easily be derived that

$$\alpha_2^{^1D_2}(J'=1)/\alpha_0^{^1D_2}(J'=1)=-1\ ,$$

$$\alpha_2^{^1D_2}(J'=2)/\alpha_0^{^1D_2}(J'=2)=+1\ ,$$

and

$$\alpha_2^{^1D_2}(J'=3)/\alpha_0^{^1D_2}(J'=3)=-2/7\ .$$

Here $\alpha^{^1D_2}(J')$ designates the sum of the contributions of a number of states with total angular momentum J' to the polarizability of the $^1D_2$ state. In Fig. 2 we have plotted $\Delta\alpha_0$ and $-\frac{7}{2}\Delta\alpha_2$ in a way similar to Fig. 1. The good agreement between the two sets of points confirms the assumption.

TABLE II. Experimental and calculated polarizabilities for $^1D_2$ states in barium. $\alpha_0(\text{rest})$ and $\alpha_2(\text{rest})$ are defined in Eq. (5).

	Scalar polarizabilities [MHz/(V/cm)^2]			Tensor polarizabilities [MHz/(V/cm)^2]		
Level	α_0^{expt}	$\alpha_0^{\text{calc}}(\text{rest})$	α_0^{calc}	α_2^{expt}	$\alpha_2^{\text{calc}}(\text{rest})$	α_2^{calc}
$14\,^1D_2$	−0.515(20)	−0.324	−0.326	−0.371(17)	−0.311	−0.310
$15\,^1D_2$	−0.0819(27)	−0.0975	−0.0906	0.0871(26)	0.0971	0.0951
$16\,^1D_2$	−0.131(4)	−0.156	−0.143	0.142(4)	0.155	0.151
$17\,^1D_2$	−0.205(9)	−0.235	−0.208	0.218(9)	0.233	0.225
$18\,^1D_2$	−0.281(12)	−0.345	−0.270	0.325(11)	0.341	0.320
$19\,^1D_2$	1.53(5)	−0.493	1.54	−0.080(24)	0.486	−0.094
$20\,^1D_2$	−0.636(20)	−0.689	−0.681	0.684(22)	0.677	0.675
$21\,^1D_2$	−0.680(26)	−0.945	−0.682	0.89(3)	0.922	0.847
$22\,^1D_2$	−0.316(15)	−1.28	−0.303	1.04(3)	1.23	0.957
$23\,^1D_2$	3.75(11)	−1.76	3.82	0.101(5)	1.58	−0.009
$24\,^1D_2$	−10.7(3)	−2.39	−10.9	4.55(14)	2.07	4.50
$25\,^1D_2$	−8.81(26)	−3.75	−8.02	4.11(14)	2.53	3.75
$26\,^1D_2$	−12.8(4)	−8.79	−10.9	4.07(13)	2.74	3.36
$5d7d\,^1D_2$	19.2(6)	10.4	11.7	−3.33(18)	−0.167	−0.528
$27\,^1D_2$	−0.876(28)	−0.856	−1.57	0.895(28)	0.909	1.11
$28\,^1D_2$	−4.44(14)	−2.56	−5.17	3.14(9)	2.53	3.28
$29\,^1D_2$	−7.1(3)	−3.76	−7.83	4.99(28)	3.73	4.90
$30\,^1D_2$	−9.6(3)	−4.83	−10.32	6.65(21)	4.81	6.38

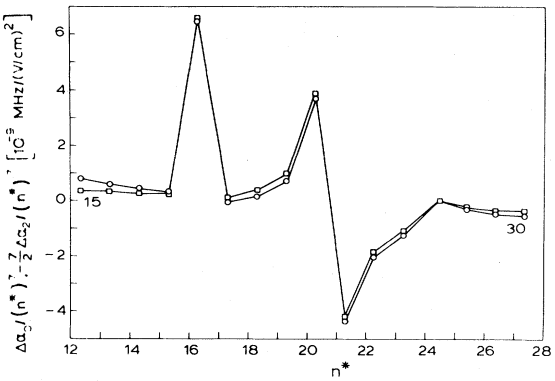

FIG. 2. Contributions of the $^1F_3$ states to the scalar $[\Delta\alpha_0/(n^*)^7]$ and tensor $[\Delta\alpha_2/(n^*)^7]$ polarizabilities as a function of n^* as calculated from the experimental results for the $^1D_2$ states of barium. □, $\Delta\alpha_0/(n^*)^7$; ○, $-\frac{7}{2}\Delta\alpha_2/(n^*)^7$.

C. MQDT analysis of the $^1F_3$ contributions

Figure 2 now also provides a general idea of the location of the $^1F_3$ states with respect to the $^1D_2$ states. Between the $6s23d\ ^1D_2$ and $6s24d\ ^1D_2$ states, the $^1F_3$ series crosses the $^1D_2$ series [the sign change corresponds to the sign change in the energy denominator of the dominant $^1F_3$ contributions in expressions (2) and (3)]. Just above the $6s19d\ ^1D_2$ state, a relatively isolated $^1F_3$ state has to be located which must, however, possess at least some $6snf\ ^1F_3$ character to cause a non-negligible dipole matrix element with the $6s19d\ ^1D_2$ state. At the low and high end of the plot, the curve levels off, indicating that the separation between the $^1F_3$ and $^1D_2$ states (expressed in n^*) becomes approximately constant. These features can only be explained by assuming at least two perturbers in the $^1F_3$ series; one weakly interacting (corresponding to the isolated state near the $6s19d\ ^1D_2$ state) and one more strongly interacting (causing the more gradual crossing near $n^*=21$ between the $6s23d\ ^1D_2$ and $6s24d\ ^1D_2$ states).

On the basis of these qualitative observations, a rough sketch of the $^1F_3$ series has been constructed which serves to generate starting values for a three-channel quantum-defect—theory analysis. Both perturbers are assumed to belong to $5dnl$ series, and the average of the two $5d$ limits has been taken as their ionization limit. The direct interaction between the two perturber channels has not been considered. The eigenquantum detects μ_α, and the two remaining interaction angles θ_i, assumed to be energy independent, are varied in a least-squares-fitting routine, not, as usual, to reproduce experimental level energies, but to reproduce $\Delta\alpha_0$ and $\Delta\alpha_2$. (For the definition of the parameters, see e.g., Ref. 28). The contributions of the $^1F_3$ states are calculated along the lines given in Sec. III B.

The resulting best-fit calculated values for the total polarizabilities are included in Table II. Figure 3 shows the experimental and best-fit theoretical values for the polarizabilities of the states included in the fit. The largest deviations are observed for states in the vicinity of the $5d7d\ ^1D_2$ perturber where a number of channels contribute to the $^1D_2$ wave functions. In general, the agreement is quite satisfactory. The final MQDT parameter set for the $^1F_3$ series is given in Table III.

D. Discussion of the MQDT analysis of the $^1F_3$ series

The identification of the two perturbers on the basis of the available data is difficult. Possible perturbers include $5d4f$ and $5d8p$, $J=3$ states. However, inspection of the known positions of $5d4f$, $J=1$ states[17] suggests that the $5d4f$, $J=3$ states lie below the studied energy range. Our best guess, based on a comparison with the $5d7p$, $J=3$ states tabulated by Moore,[29] is $5d8p\ ^1F_3$ for the perturber associated with channel 2 and $5d8p\ ^3D_3$ for the one associated with channel 3 (near $6s19d\ ^1D_2$). The identification of the perturbers does not affect the calculation of the polarizabilities, as only the $6snf$ fraction in their wave functions contributes significantly to the dipole matrix elements.

The tentative MQDT analysis which is presented here can, of course, not be compared with a regular MQDT analysis based on experimental level energies. Certainly the predictive power outside the studied energy range is limited, if only because of the presence of other perturbers (e.g., the $5d4f$, $J=3$ states), presumably below the ionization limit, which have not been considered. It is, nevertheless, worthwhile to compare calculated level energies within the studied range with the scarce existing data. In Fig. 4 a partial Lu-Fano plot is shown of states considered in this work. The triangles correspond to the $^1D_2$ states and the circles to the $^1F_3$ states as calculated with the parameters of Table III. The squares correspond to the $^3F_3$ states and are included to aid the discussion hereafter.

On the left (low-energy) side of Fig. 4, the approximate energy of the $6s12f\ ^1F_3$ state which can be extracted from the data of Zimmerman *et al.*,[22] is indicated with a cross. In a two-step excitation setup similar to the one used in the present experiment, the $6s12f\ ^1F_3$ state was observed through mixing with $6snd$ states in a strong (>1 kV/cm) electric field. The approximate energy from Fig. 1 of Ref.

TABLE III. Parameters of the tentative three channel MQDT analysis of the $^1F_3$ series. The errors correspond to 67% confidence intervals.

Channel Label		1 $6snf\ ^1F_3$	2 $5d8p\ ^1F_3$	3 $5d8p\ ^3D_3$
	E_{ion} (cm^{-1})	42 034.95	47 309.0	47 309.0
	μ_α	0.08(4)	0.5571(9)	0.6084(5)
	θ_1	0.26(2)	Couples 1 and 2	
	θ_2	0.17(3)	Couples 1 and 3	

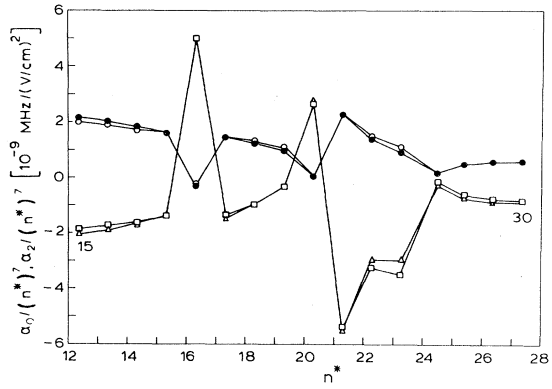

FIG. 3. Experimental and calculated values of $\alpha_0/(n^*)^7$ and $\alpha_2(n^*)^7$ as a function of n^* for barium $^1D_2$ states. □, α_0^{expt}; △, α_0^{calc}; ○, α_2^{expt}; ●, α_2^{calc}.

22 is 41 260 cm^{-1}. The deviation from the calculated level energy amounts to 0.05 to n^*.

The crosses on the right-hand side of Fig. 4 do not correspond to measured level energies. They represent the positions of the $6snf\,^1F_3$ states with $n=19$, 21, 22, 25, 30, and 31 as calculated from the parametric analysis of the hyperfine structure in the corresponding ^3F states of the odd barium isotopes.[19] For $n \geq 21$, the present analysis agrees with the general trend in these data points (the broken line in Fig. 4), although it shows a steeper slope. At $n=19$, the trend in the data points shows a sharp bend, in clear disagreement with the present results.

The parametric analysis of Eliel and Hogervorst[19] is strictly valid only if the $^1F_3$ series is unperturbed (as well as the ^3F series). This assumption cannot be maintained for the $6snf$ states with $n \leq 30$, even considering only the results of the hyperfine-structure analysis itself (viz., Fig. 4).

The overestimation of the singlet-triplet splitting apparent in Fig. 4 for the $6snf$ states with n between 22 and 30 (assuming the present analysis to be correct) can easily be explained. In the hyperfine-structure analysis, the energies of the $^1F_3$ states are deduced from the repulsion, induced by the spin-orbit and hyperfine interactions, of

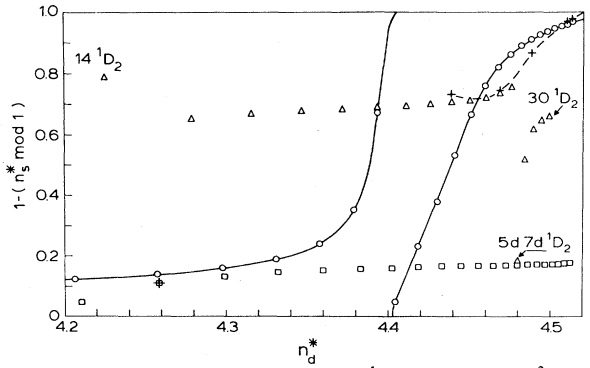

FIG. 4. Partial Lu-Fano plot of $^1D_2$ states (△), $^3F_3$ states (□), and calculated $^1F_3$ states (○). (+); $^1F_3$ states from Refs. 19 and 22. The broken curve through these points serves to guide the eye.

$6snf\,^3F$ hyperfine-structure sublevels by $6snf\,^1F$ sublevels with the same total angular momentum. The thus calculated $^1F_3$-$^3F_3$ energy differences will only be correct if the perturber fraction in the $6snf$ states is negligible and all splittings within the $6snf$ configuration are much smaller than the difference in average energy between the $6snf$ and $6s(n\pm1)f$ configurations. Between $n=22$ and 30 the perturber fraction in the $6snf\,^1F$ states, according to our tentative MQDT analysis, does not exceed a few percent, so that the first condition is approximately fulfilled. However, the singlet-triplet splitting increases to such an extent that it becomes comparable to the $6snf\,^3F$-$6s(n-1)f\,^1F$ energy separation. The repulsion of $6snf\,^3F$ hyperfine sublevels by $6snf\,^1F$ sublevels (higher in energy) is counteracted by the repulsion by the corresponding $6s(n-1)f\,^1F$ hyperfine sublevels (lower in energy). The experimentally observed decrease in the repulsion is interpreted in the hyperfine analysis by overestimating the singlet-triplet splitting.

Near $n=20$, the ^3F states are positioned just between two consecutive states of the ^1F sequence, and the perturber fraction in the singlet states reaches a maximum of 15%. The parametric hyperfine-structure analysis cannot be expected to yield any meaningful result in this region.

From the preceding analysis it follows that the identification of the $6snf\,^1F_3$ level reported by Gallagher *et al.*[8] is inconsistent with the present results as well as with the hyperfine-structure results. The values of the polarizabilities of the $5d7d\,^1D_2$ state suggest that the observed rf transition is from $5d7d\,^1D_2$—$6s24f\,^3F_3$ instead.

As a final remark in this section, the combination of an almost unperturbed ^3F series and a heavily perturbed ^1F series is not surprising. Generally, configuration interaction in alkaline-earth atoms is much stronger in singlet than in triplet series.[30]

IV. CONCLUSION

In the present work we have utilized low-field Stark-effect measurements of the $6snd\,^1D_2$ states in barium to extract information on the unknown $6snf\,^1F_3$ series. The results indicate the feasibility of Stark-effect calculations for highly perturbed Rydberg series by combining wave functions evaluated from MQDT analyses and radial integrals calculated in the Coulomb approximation. Furthermore, a wider applicability of Stark-effect data than is usually brought into practice is demonstrated. A comparison with the results of hyperfine-structure measurements in the $6snf\,^3F$ states suggests a partial explanation for the behavior of the latter results at low n, in terms of a perturbed $^1F_3$ series.

The final test of the present approach is, of course, the direct measurements of the $^1F_3$ level positions, which is feasible, e.g., by absorption measurements from the metastable $6s5d\,^1D_2$ state. Such an experiment is in progress in our laboratory.

ACKNOWLEDGMENTS

We wish to thank M. Aymar for making available her unpublished data and M. L. Zimmerman for his computer code. The Stichting voor Fundamenteel Onderzoek der Materie is gratefully acknowledged for financial support.

*Present address: Dr. Neher Laboratorium, St. Paulusstraat 4, Leidschendam, The Netherlands.
[1]D. J. Bradley, P. Ewart, J. V. Nicholas, and J. R. D. Shaw, J. Phys. B 6, 1594 (1973).
[2]J. R. Rubbmark, S. A. Borgström, and K. Bockasten, J. Phys. B 10, 421 (1977).
[3]M. Aymar, P. Camus, M. Dieulin, and C. Morillon, Phys. Rev. A 18, 2173 (1978).
[4]P. Camus, M. Dieulin, and A. El Himdy, Phys. Rev. A 26, 379 (1982).
[5]M. Aymar and O. Robaux, J. Phys. B 12, 531 (1979).
[6]M. Aymar and P. Camus, Phys. Rev. A (in press).
[7]K. Bhatia, P. Grafström, C. Levinson, H. Lundberg, L. Nilsson, and S. Svanberg, Z. Phys. A 303, 1 (1981).
[8]T. F. Gallagher, W. Sandner, and K. A. Safinya, Phys. Rev. A 23, 2969 (1981).
[9]M. Aymar, R.-J. Champeau, C. Delsart, and J. C. Keller, J. Phys. B 14, 4489 (1981).
[10]P. Grafström, C. Levinson, H. Lundberg, S. Svanberg, P. Grundevik, L. Nilsson, and M. Aymar, Z. Phys. A 308, 95 (1982).
[11]W. Hogervorst and E. R. Eliel, Z. Phys. A 310, 19 (1983).
[12]P. Grafström, Jiang Zhan-Kui, G. Jönsson, S. Kröll, C. Levinson, H. Lundberg, and S. Svanberg, Z. Phys. A 306, 281 (1982).
[13]J. Neukammer and H. Rinneberg, J. Phys. B 15, L723 (1982).
[14]H. Rinneberg and J. Neukammer, Phys. Rev. A 27, 1779 (1983).
[15]E. R. Eliel and W. Hogervorst, J. Phys. B 16, 1881 (1983).
[16]M. Aymar (private communication).
[17]J. A. Armstrong, J. J. Wynne, and P. Esherick, J. Opt. Soc. Am. 69, 211 (1979).
[18]J. L. Carlsten, T. J. McIlrath, and W. H. Parkinson, J. Phys. B 8, 38 (1975).
[19]E. R. Eliel and W. Hogervorst, Phys. Rev. A 27, 2995 (1983).
[20]B. Fechner, P. Kulina, and R.-H. Rinkleff, Z. Phys. A 307, 375 (1982).
[21]D. R. Bates and A. Damgaard, Philos. Trans. R. Soc. London 242, 101 (1949).
[22]M. L. Zimmerman, Th. W. Ducas, M. G. Littman, and D. Kleppner, J. Phys. B 11, L11 (1978).
[23]C. Fabre and S. Haroche, Opt. Commun. 15, 254 (1975).
[24]J. R. P. Angel and P. G. H. Sandars, Proc. R. Soc. London, Ser. A 305, 125 (1968).
[25]K. A. H. van Leeuwen and W. Hogervorst (unpublished).
[26]M. L. Zimmerman, M. G. Littman, M. M. Kash, and D. Kleppner, Phys. Rev. A 20, 2251 (1979).
[27]M. L. Zimmerman (private communication).
[28]C.-M. Lee and K. T. Lu, Phys. Rev. A 8, 1241 (1973).
[29]C. E. Moore, *Atomic Energy Levels, National Stand. Ref. Data Ser.* (National Bureau of Standards, Washington, D.C., 1971), Vol. III.
[30]J. J. Wynne and J. A. Armstrong, IBM J. Res. Dev. 23, 490 (1979).